Online Supplementary Material: Distribution Metric

A. Glocer[1], L. Rastätter[1], M. Kuznetsova[1], A. Pulkkinen[1], H. J. Singer[6], C.

Balch[6], D. Weimer[2], D. Welling[4], M. Wiltberger[3], J. Raeder[5] and R. Weigel[7],

J. McCollough[8], S. Wing[9]

————

[1]NASA Goddard Space Flight Center,

Greenbelt, MD 20771, USA.

[2]Center for Space Science and

Engineering Research, Virginia Polytechnic

Institute and State University, Blacksburg,

Virginia, USA.

[3]High Altitude Observatory, National

Center for Atmospheric Research, Boulder,

Colorado, USA.

[4]Department of Atmospheric, Oceanic,

and Space Sciences, University of Michigan,

USA.

[5]Space Science Center & Physics

Department, University of New Hampshire,

USA.

Abstract.

This document contains the online suplementary material. Specifically the distribution metric for each model.

[6]Space Weather Prediction Center,

NOAA, Boulder, Colorado, USA.

[7]Department of Computational and Data

Sciences, George Mason University, Fairfax,

Virginia, USA.

[8]Air Force Research Laboratory,

Albuquerque, NM, USA.

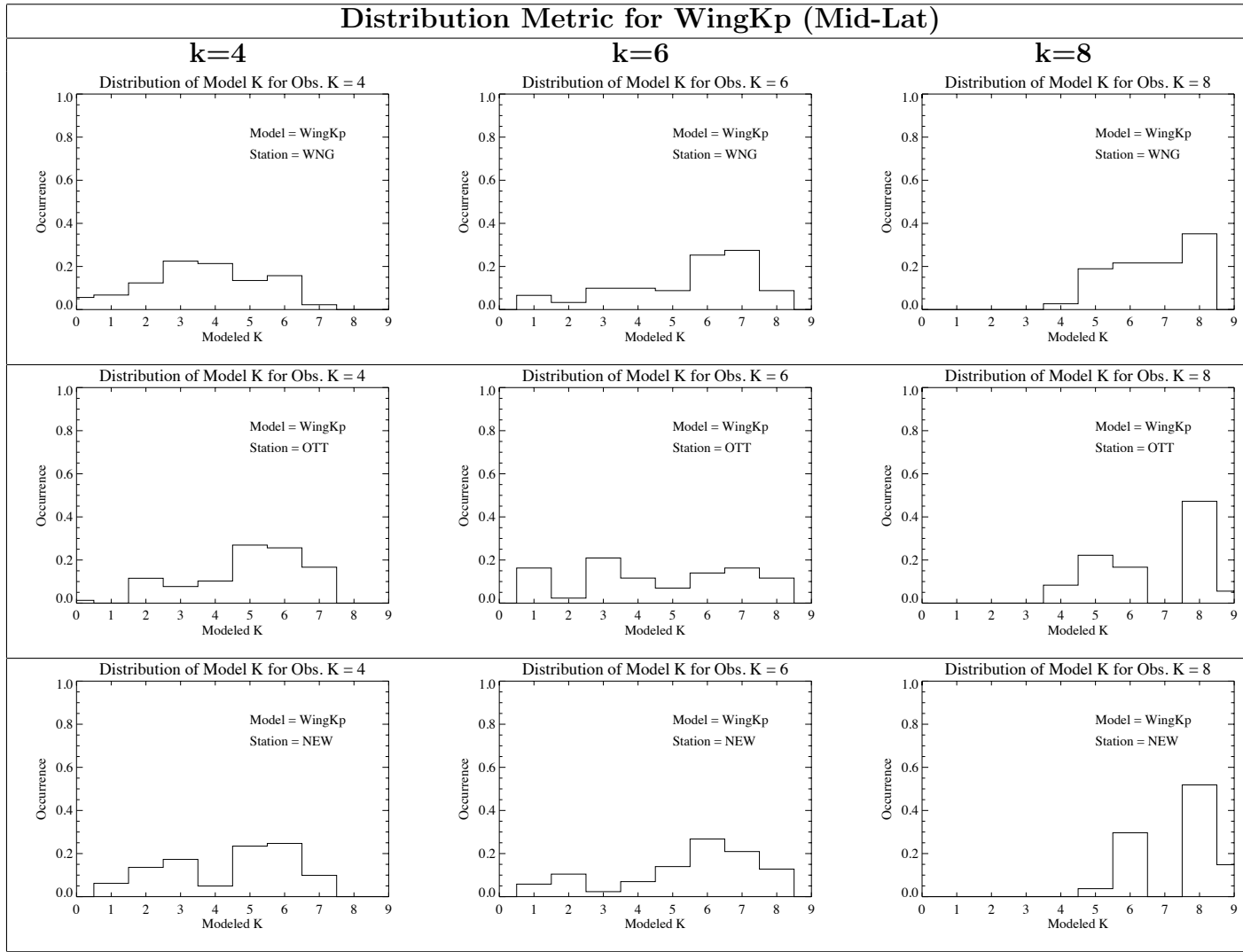[9]Johns Hopkins University Applied

Physics Laboratory, Laurel, Maryland, USA

Figure 1. Distribution of WingKp Model predictions when K=4 (left column), K=6 (middle column), and K=8 (right column). Each row presents results for a different mid-latitude station.
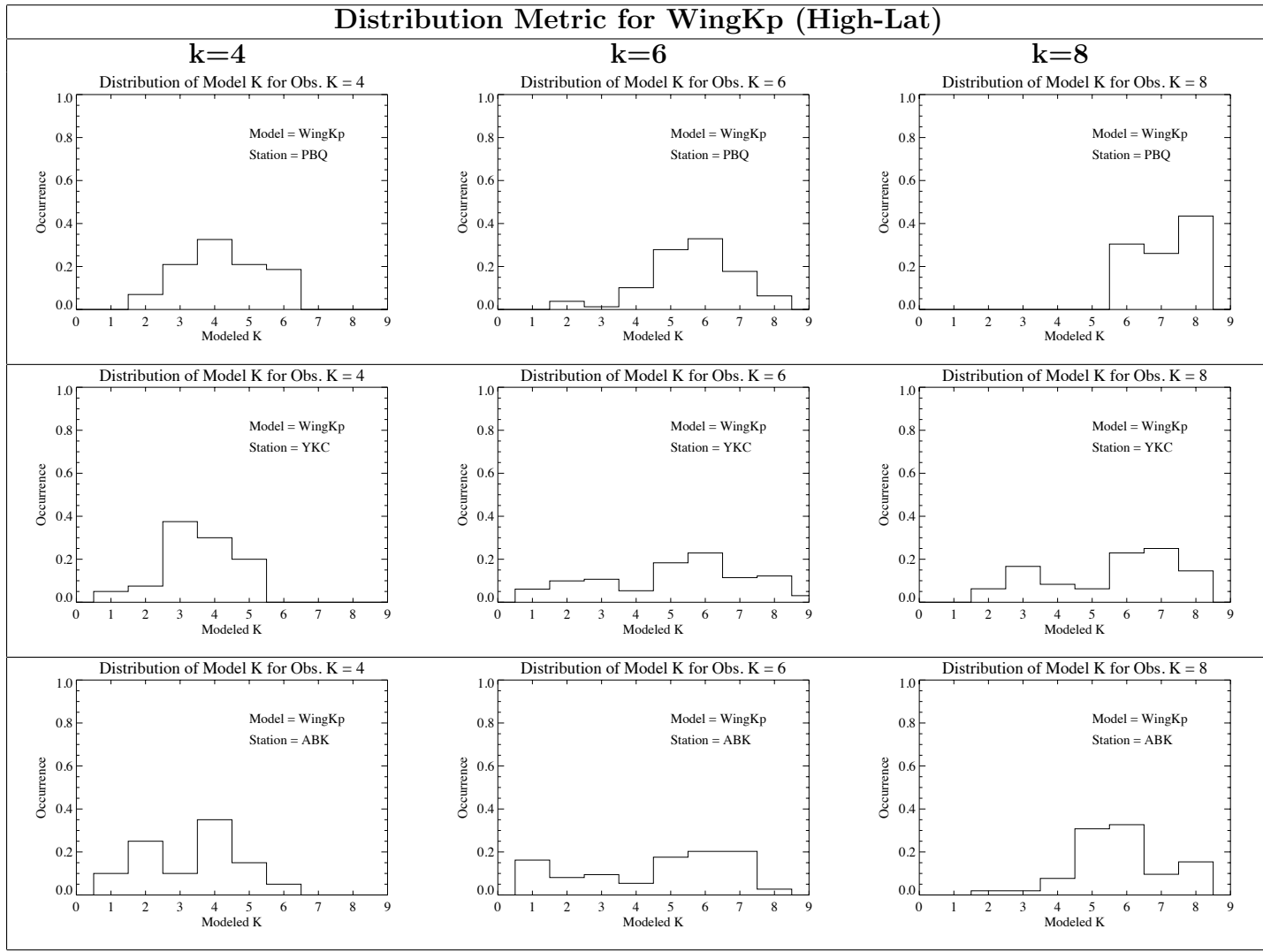
Figure 2. Distribution of WingKp Model predictions when K=4 (left column), K=6 (middle column), and K=8 (right column). Each row presents results for a different high-latitude station.
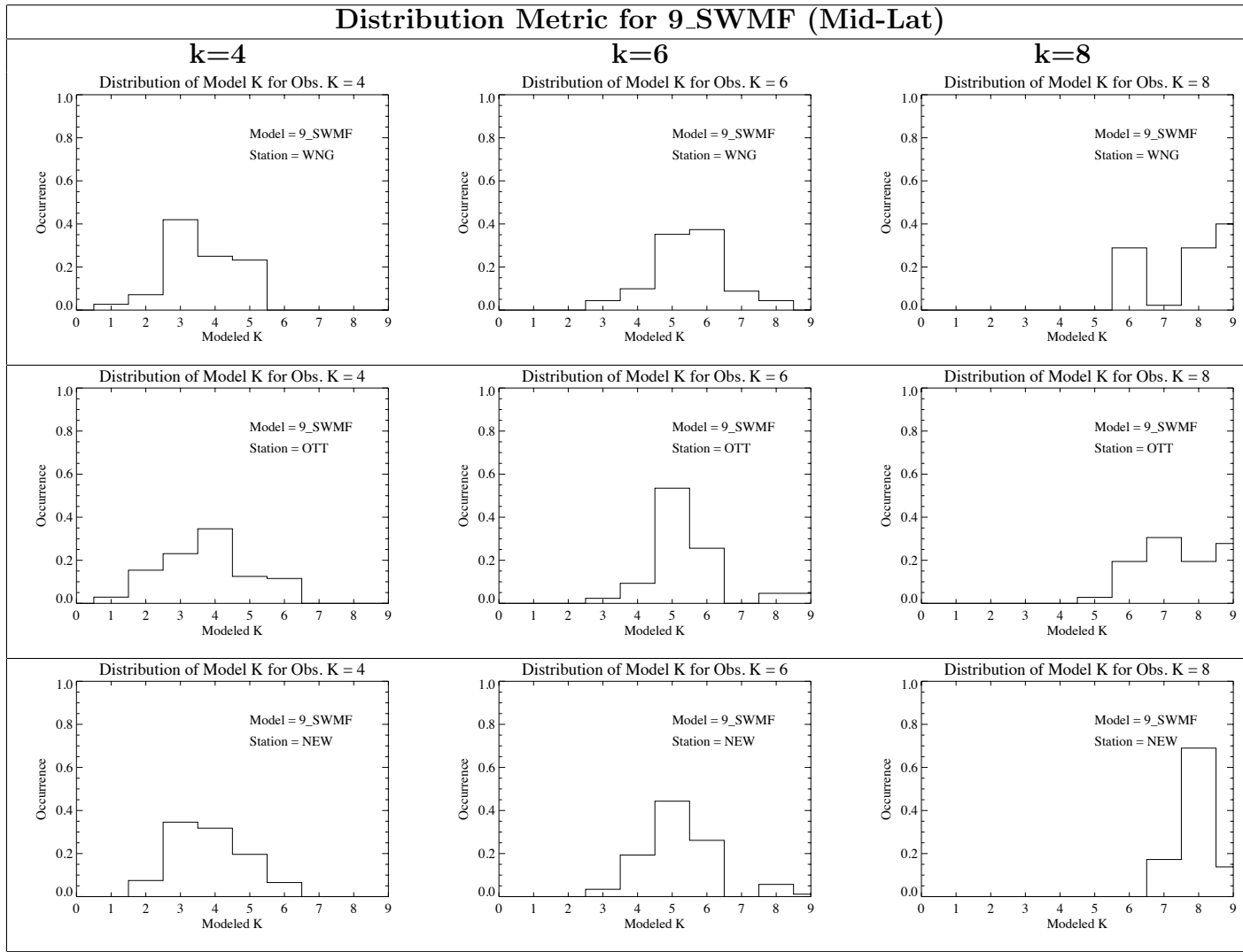
Figure 3. Distribution of 9_SWMF Model predictions when K=4 (left column), K=6 (middle column), and K=8 (right column). Each row presents results for a different mid-latitude station.
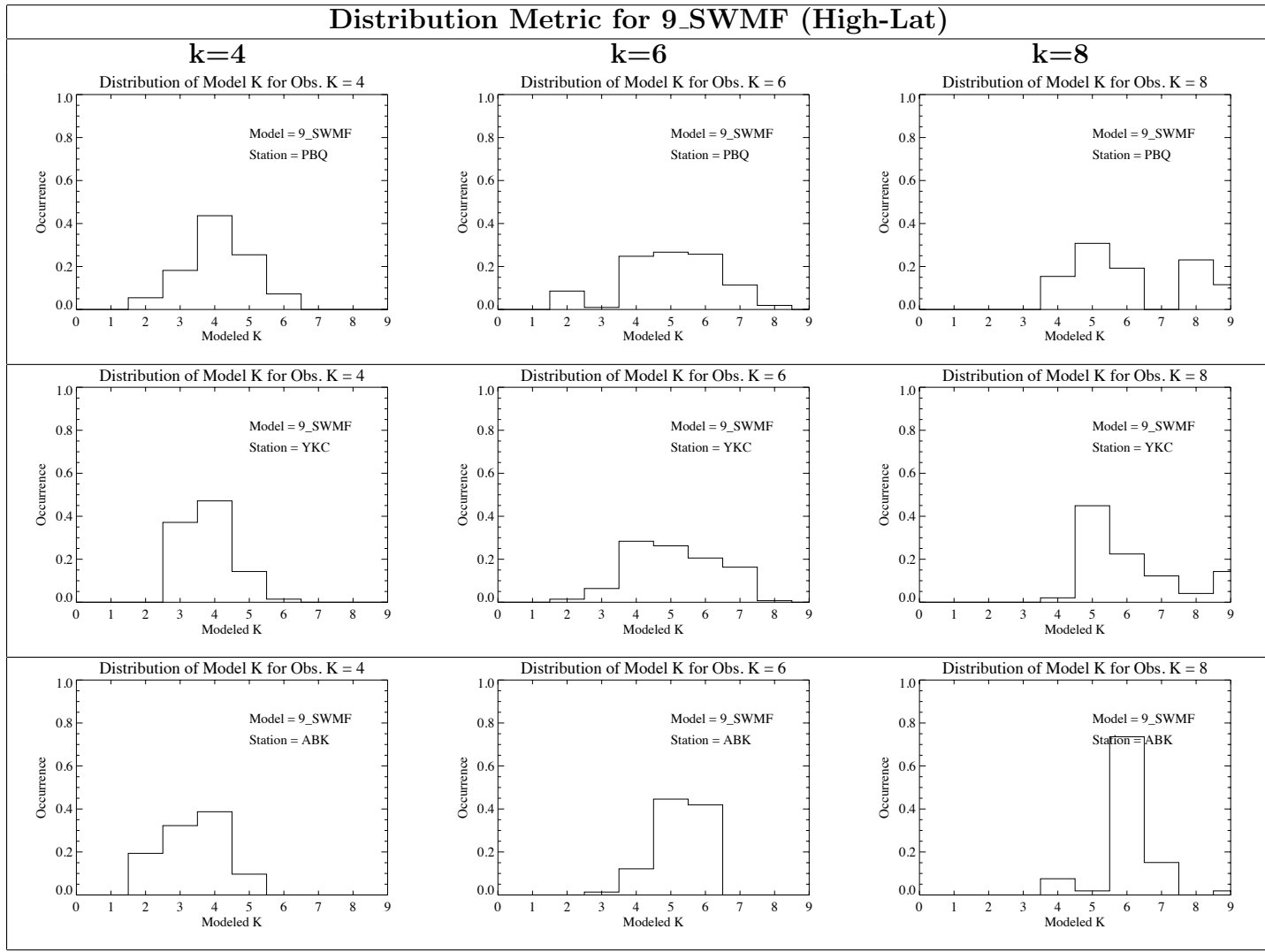
Figure 4. Distribution of 9_SWMF Model predictions when K=4 (left column), K=6 (middle column), and K=8 (right column). Each row presents results for a different high-latitude station.
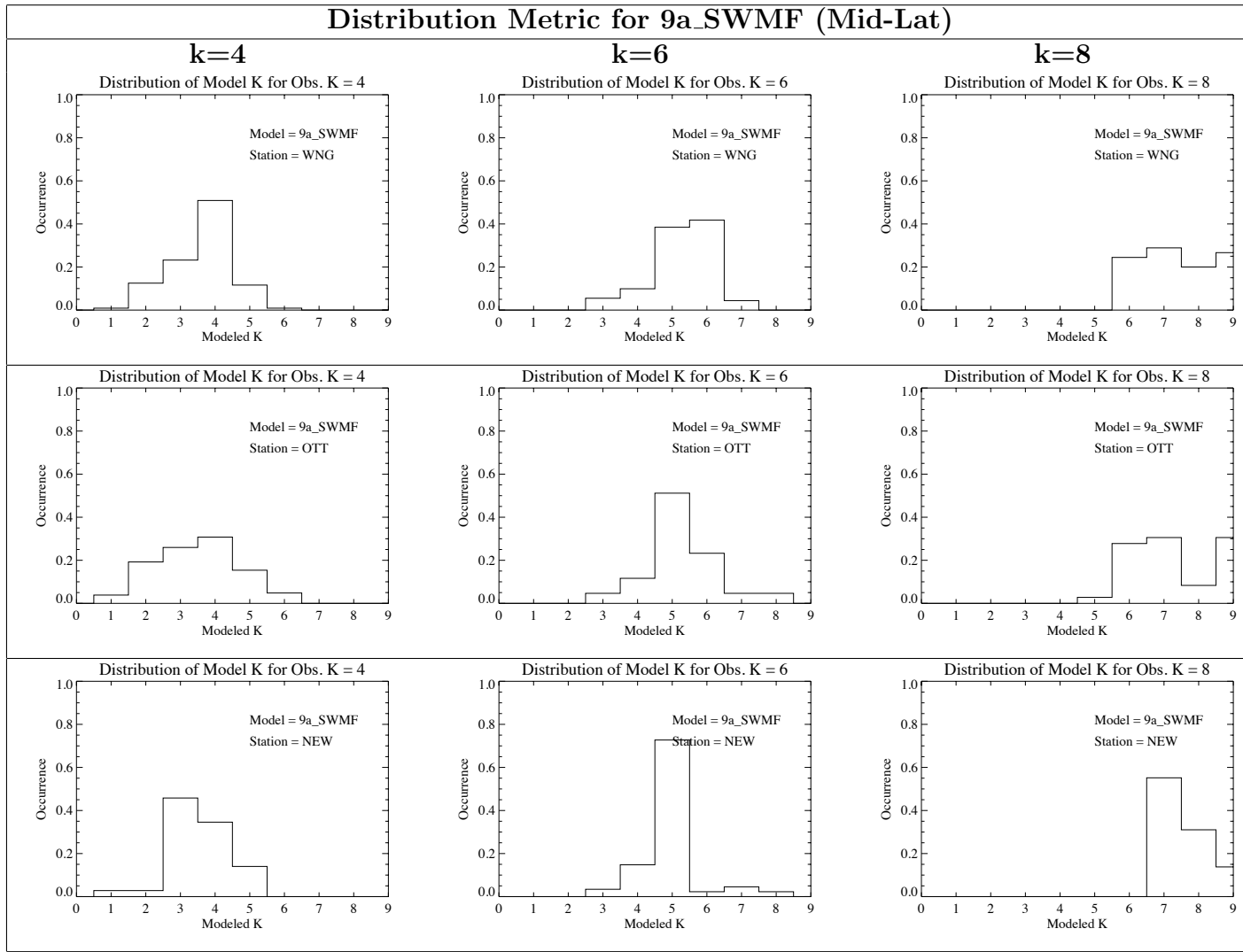
Figure 5. Distribution of 9a_SWMF Model predictions when $K=4$ (left column), $K=6$ (middle column), and $K=8$ (right column). Each row presents results for a different mid-latitude station.
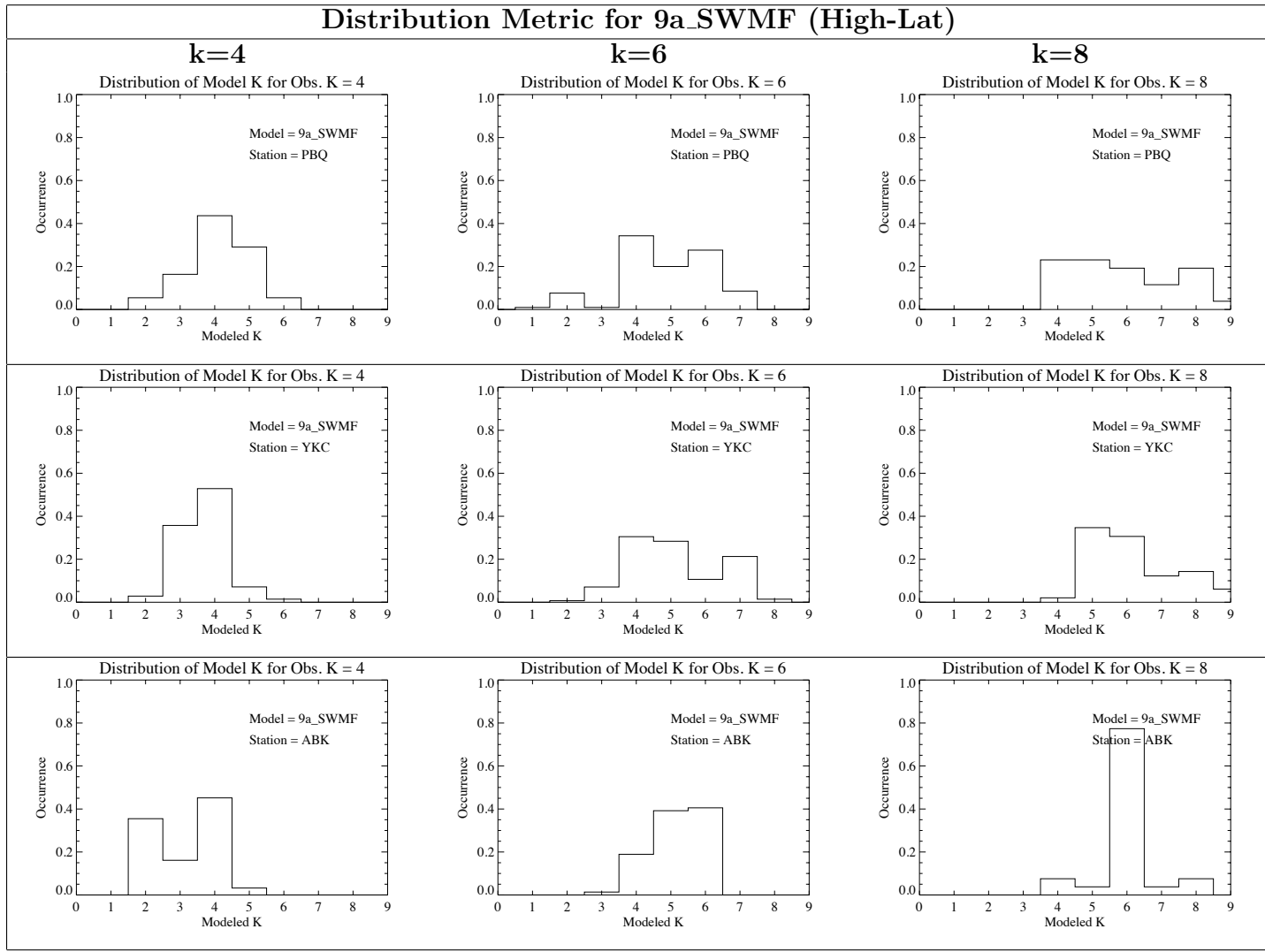
Figure 6. Distribution of 9a_SWMF Model predictions when $K=4$ (left column), $K=6$

(middle column), and $K=8$ (right column). Each row presents results for a different
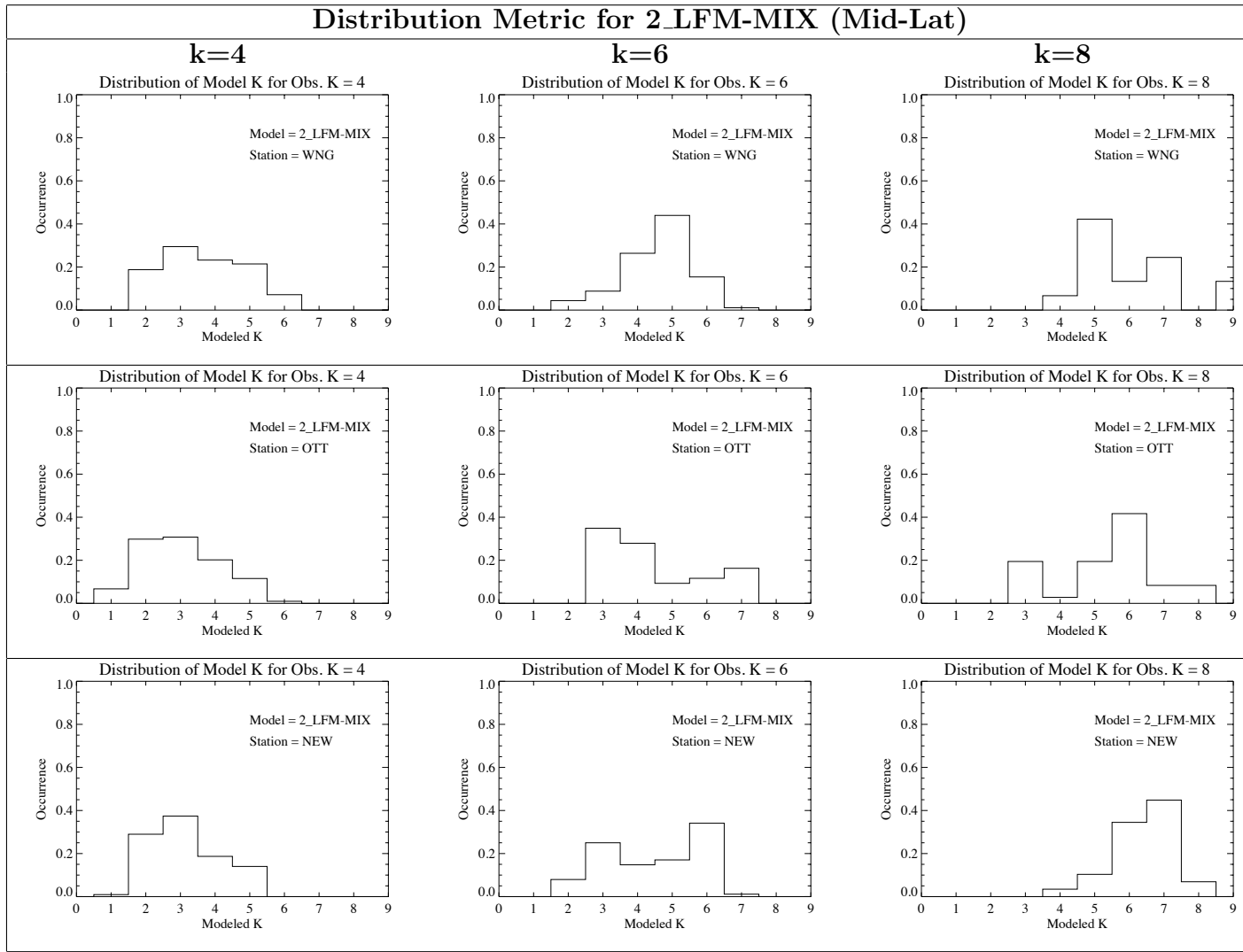
high-latitude station.

Figure 7. Distribution of 2_LFM-MIX Model predictions when K=4 (left column),

K=6 (middle column), and K=8 (right column). Each row presents results for a different
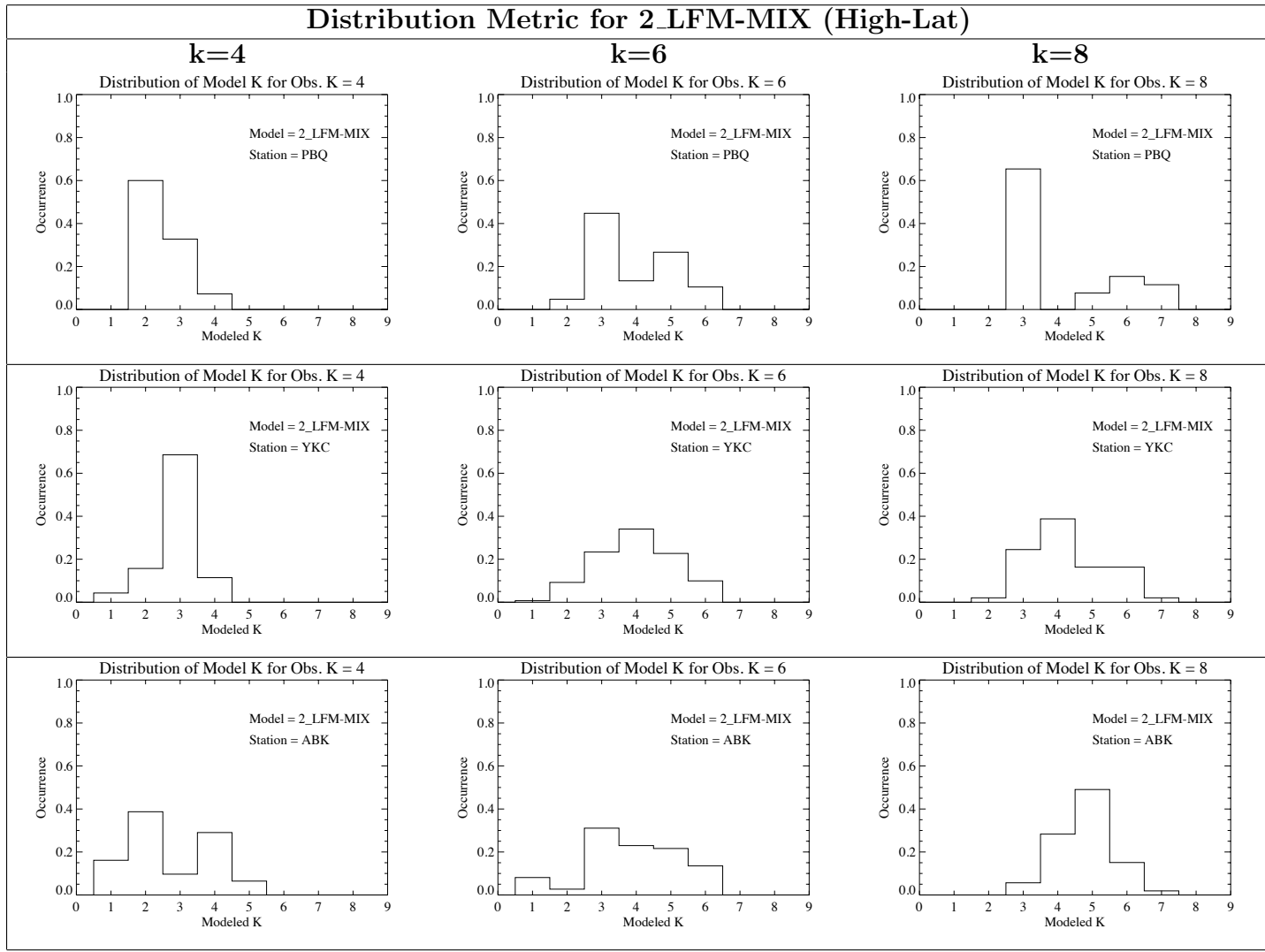
mid-latitude station.

Figure 8. Distribution of 2_LFM-MIX Model predictions when $K=4$ (left column), $K=6$ (middle column), and $K=8$ (right column). Each row presents results for a different high-latitude station.
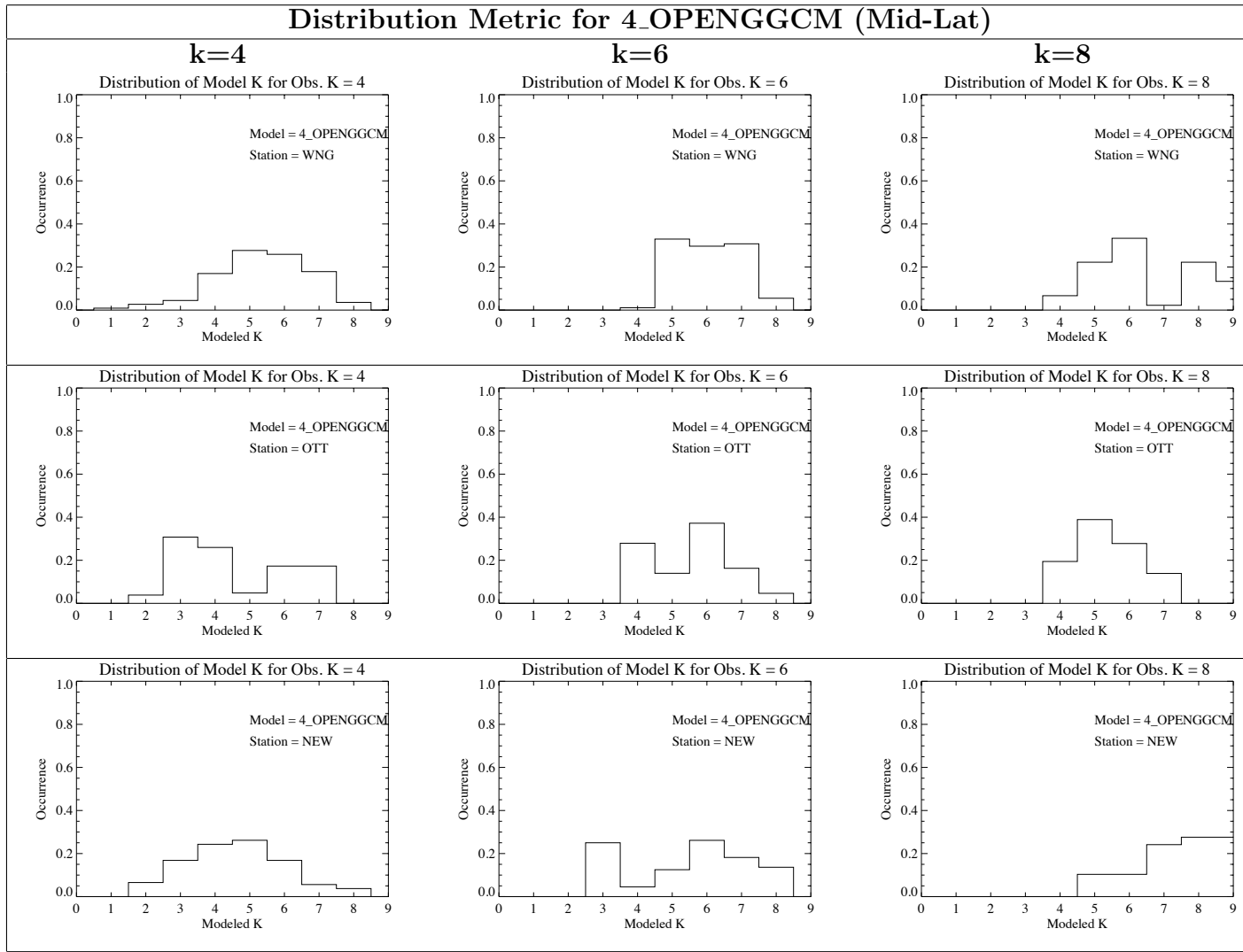
Figure 9. Distribution of 4_OPENGGCM Model predictions when K=4 (left column),

K=6 (middle column), and K=8 (right column). Each row presents results for a different
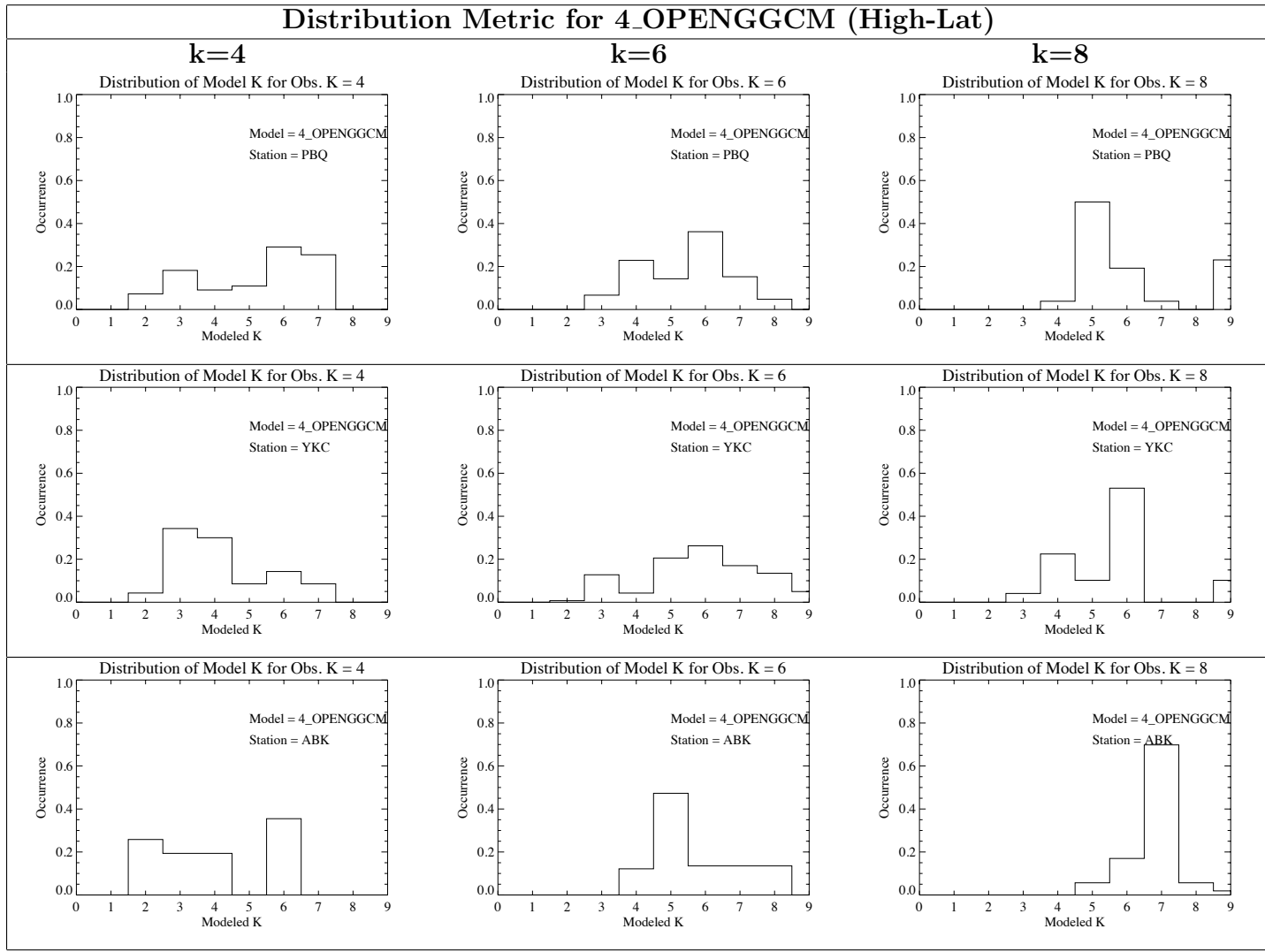
mid-latitude station.

Figure 10.   Distribution of 4_OPENGGCM Model predictions when K=4 (left column),

K=6 (middle column), and K=8 (right column). Each row presents results for a different
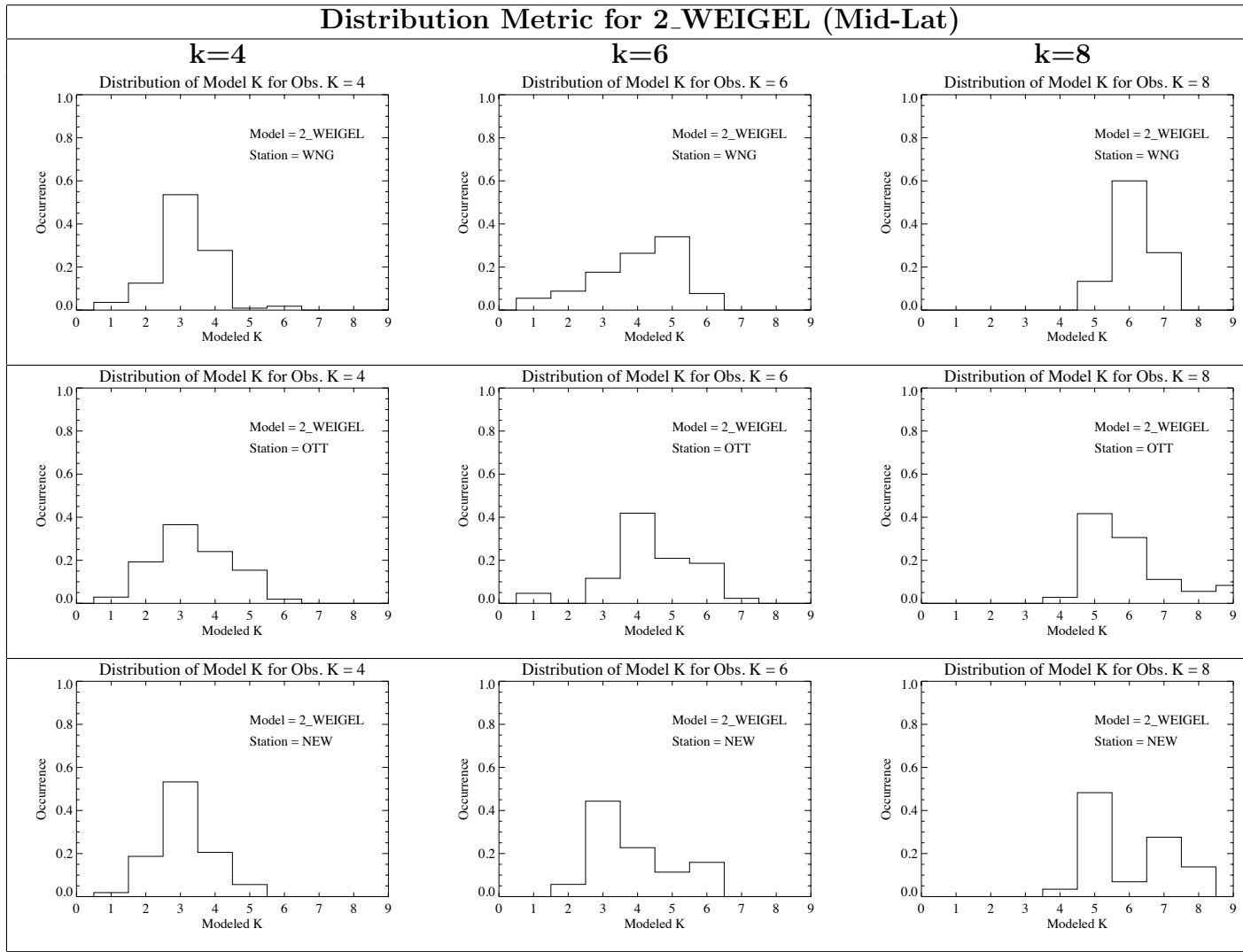
high-latitude station.

Figure 11. Distribution of 2_WEIGEL Model predictions when K=4 (left column), K=6 (middle column), and K=8 (right column). Each row presents results for a different mid-latitude station.
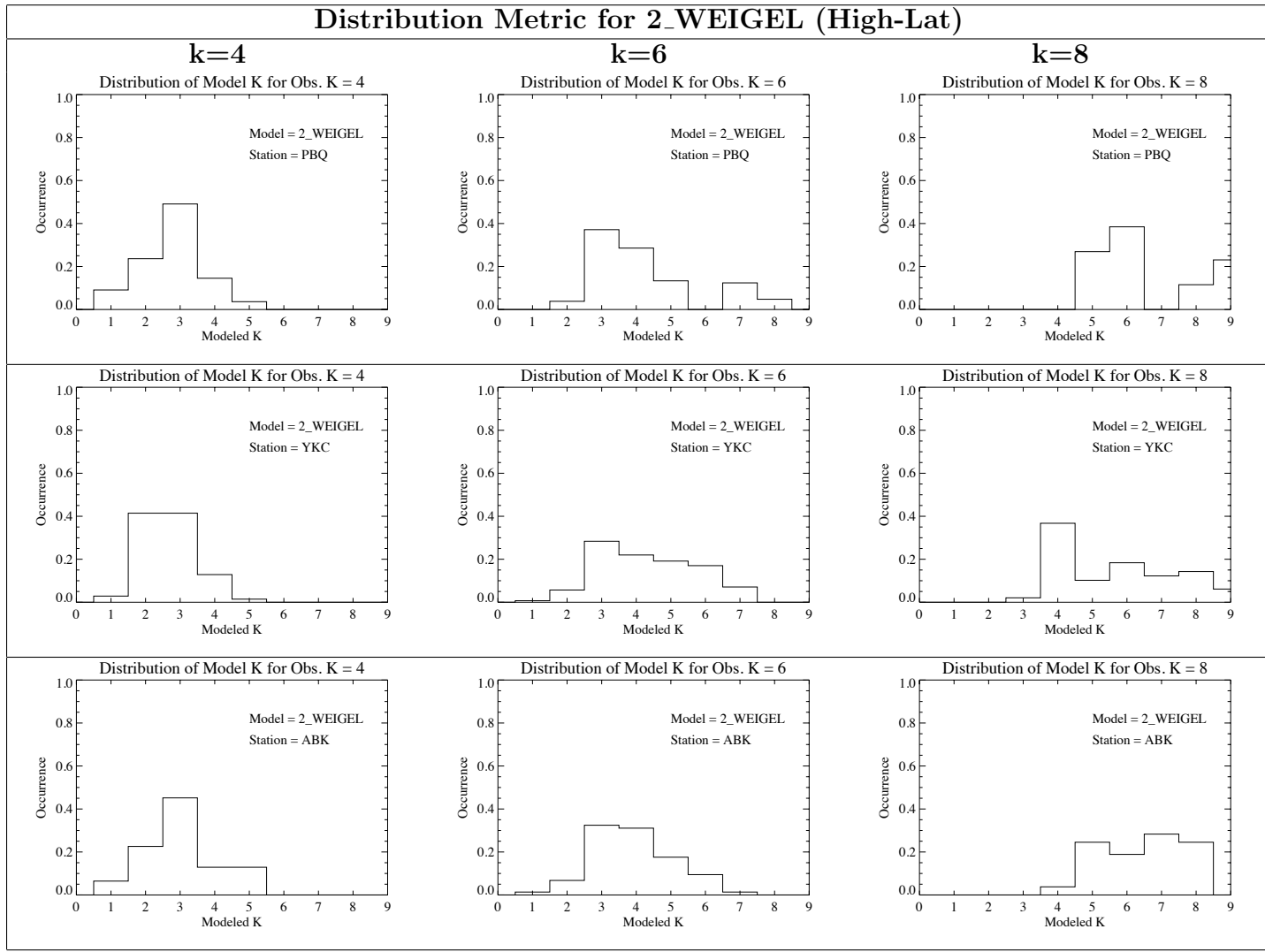
Figure 12. Distribution of 2_WEIGEL Model predictions when K=4 (left column),

K=6 (middle column), and K=8 (right column). Each row presents results for a different
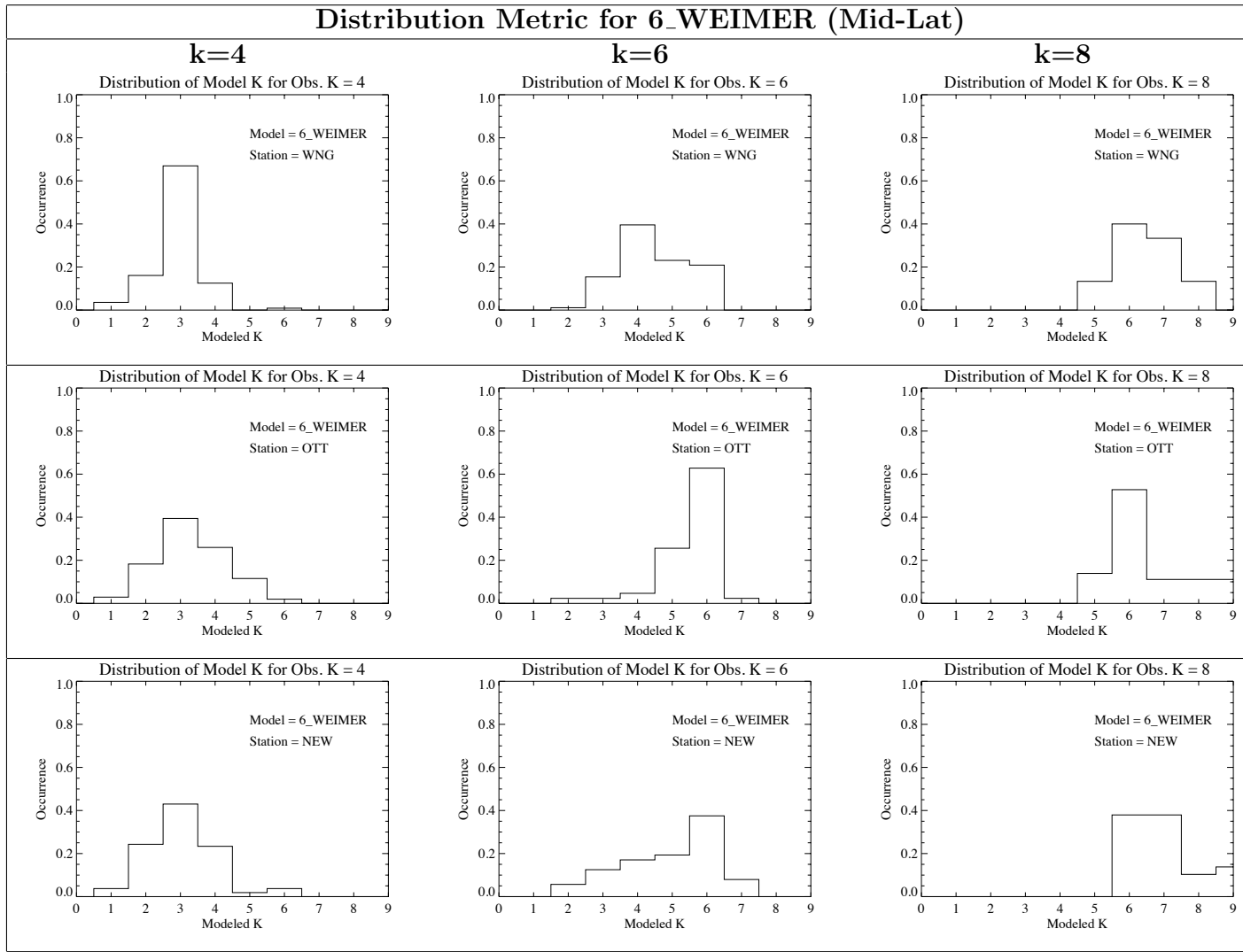
high-latitude station.

Figure 13. Distribution of 6_WEIMER Model predictions when K=4 (left column),

K=6 (middle column), and K=8 (right column). Each row presents results for a different
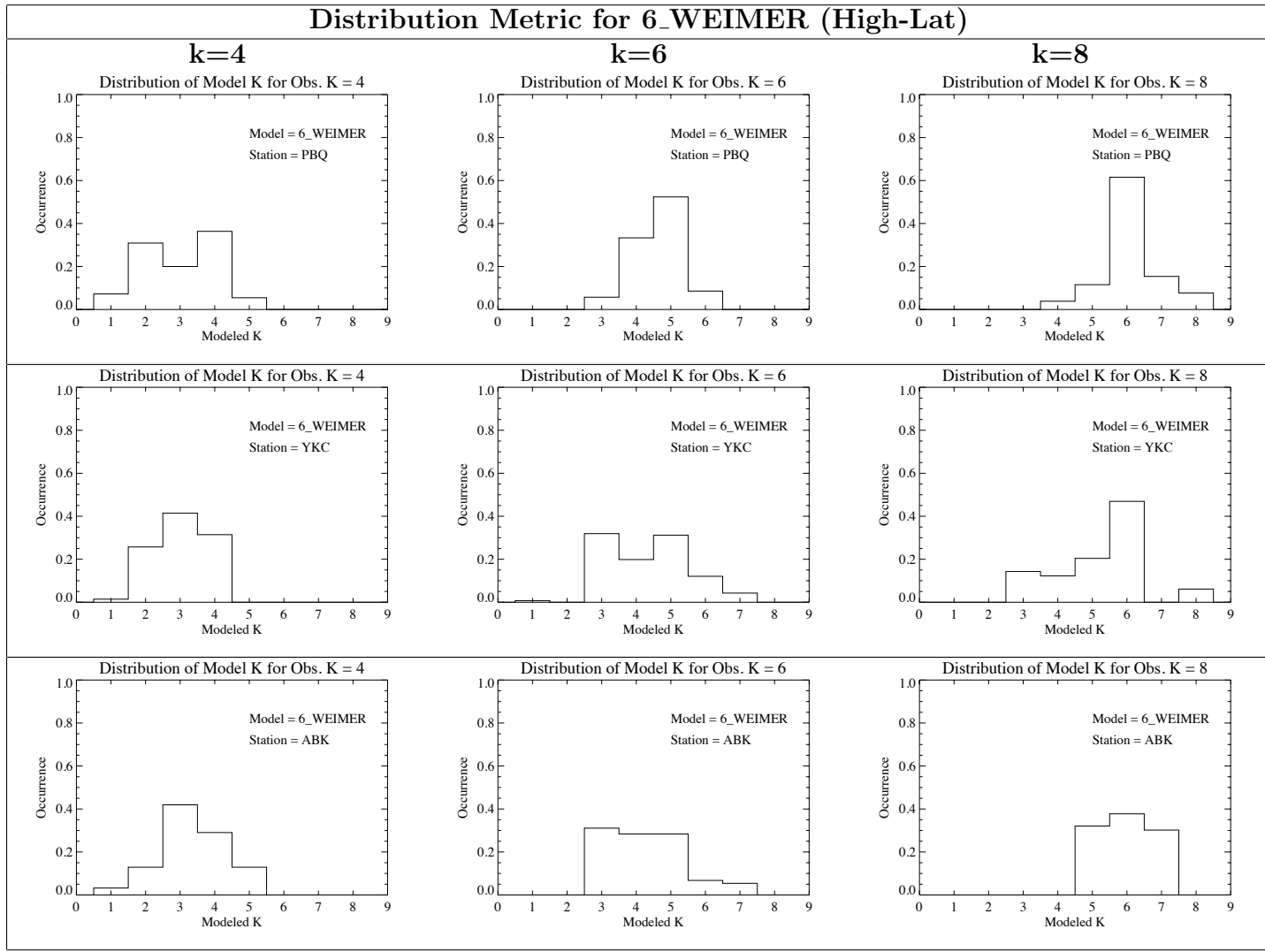
mid-latitude station.

Figure 14. Distribution of 6_WEIMER Model predictions when K=4 (left column),

K=6 (middle column), and K=8 (right column). Each row presents results for a different

high-latitude station.